EPJ Web of Conferences **17**, 08001 (2011)
DOI: 10.1051/epjconf/20111708001

Simultaneous analysis of elastic, breakup, and fusion channels for ^{6}He induced reactions at energies near the Coulomb barrier

A. M. Moro[1,a], J. P. Fernández-García[1,2], M. A. G. Alvarez[1,2], and M. Rodríguez-Gallardo[1,3]

[1] Departamento de FAMN, Universidad de Sevilla, Apartado 1065, 41080 Sevilla, Spain
[2] Centro Nacional de Aceleradores, Universidad de Sevilla, 41092 Sevilla, Spain
[3] Instituto de Estructura de la Materia, CSIC, Serrano 123, 28006 Madrid, Spain

Abstract. We present some recent applications of the Continuum-Discretized Coupled-Channels (CDCC) and Coupled-Reaction-Channels (CRC) methods to the study of reactions induced by weakly-bound nuclei on stable targets. The methods are applied to the scattering of the Borromean nucleus ^{6}He at energies around the Coulomb barrier. Elastic scattering data are very well described by four-body CDCC calculations (based on a three-body description of the ^{6}He nucleus) but also by simpler three-body CDCC calculations, using a suitable two-body model for ^{6}He. By contrast, inclusive α data are better described using the CRC approach, which treats the breakup within the transfer to the continuum picture and, unlike the CDCC method, allows the inclusion of transfer to bound states of the target. We explore also the possibility of calculating the fusion cross sections using the CRC framework.

1 Introduction

The considerable amount of experimental data of reactions induced by light exotic nuclei accumulated during the past two decades permits nowadays to establish a systematics on how the loosely-bound nature of these nuclei manifests in the different reaction observables. At energies around and below the Coulomb barrier, and for medium-mass and heavy targets, these reactions display some common and remarkable features. The elastic scattering shows a signif cant suppression with respect to the Rutherford cross section, decreasing smoothly as a function of the scattering angle, in contrast to the expected Fresnel interference pattern that characterizes the scattering of heavy ions at these energies. Moreover, these reactions exhibit a large dissociation probability (transfer/breakup). Finally, the fusion probability shows signif cant deviations with respect to the one-barrier penetration model prediction. At energies above the Coulomb barrier, most models predict a reduction of the fusion probability due to the coupling to the breakup channels. Below the barrier, the situation is more controversial and no overall consensus has been already achieved.

Clearly, all these phenomena are interrelated. For example, the effects on the elastic and fusion cross sections described above are clearly a consequence of the large coupling to the inelastic, breakup and transfer channels. Although specif c models have been developed for the different processes, we still lack a method to deal with all the relevant channels within a common framework.

[a] e-mail: moro@us.es

In this contribution we present some recent results obtained by our group in an attempt to achieve a global understanding of reactions with weakly-bound nuclei. Although the methods discussed here can be applied to other cases, we focus here on reactions induced by the Borromean nucleus ^{6}He, for which a large body of experimental data and calculations have been accumulated over the past years.

2 Elastic cross section

Elastic angular distributions for ^{6}He reactions have been measured at Coulomb barrier energies on a wide range of targets, for example, ^{27}Al [1], ^{64}Zn [2], ^{120}Sn [3], ^{208}Pb [4–6], ^{209}Bi [7,8], among others. For medium-mass and heavy targets, these angular distributions show a smooth angular dependence and a total or partial absence of the Fresnel characteristic diffraction pattern. Furthermore, the cross section starts to deviate from the Rutherford formula at relatively small angles which, in a classical picture, would correspond to distant trajectories. This behaviour, recently referred to as *long-range absorption* effect [4–6], suggests the presence of reaction mechanisms that remove f ux from the elastic channel at distances well beyond the strong absorption radius.

Given the small separation energy of the ^{6}He nucleus, it is expected that the main non-elastic channel is the dissociation of the projectile into its constituents ($\alpha + n + n$). This effect can be properly taken into account within the Continuum-Discretized Coupled-Channels (CDCC) framework [9]. In fact, CDCC calculations applied to ^{6}He scattering [10–12] have conf rmed that the long-range absorption phenomenon can be explained in terms of the strong

couplings to the breakup channels, due mainly to the dipole Coulomb interaction.

The application of the CDCC method to ^{6}He collisions deals with the difficulty that a realistic description of this nucleus requires a three-body model ($\alpha + n + n$). Since the CDCC method was originally formulated for two-body projectiles, first applications of this method to ^{6}He used a simple *di-neutron* model for this nucleus, assuming that the two halo neutrons can be treated as a structureless spin-zero cluster bound to the α core with an energy given by the two-neutron separation energy, $|\varepsilon_b|=S_{2n}=0.975$ MeV (eg. [13–15]). However, this model gives rise to a ground state wave function which extends too much in configuration space and, consequently, to an overestimation of the coupling to the continuum states [16,17]. In [17] we proposed an improved di-neutron model, which palliates this problem, while keeping the simplicity of the two-body description. The idea is to define an effective $\alpha-2n$ Hamiltonian, such that the ground state wave function reproduces in the best possible the density along the $2n$-core coordinate, when compared with a realistic three-body calculation. In particular, in order to reproduce the tail of this density, one requires an effective separation energy of $\varepsilon_b \simeq -1.6$ MeV. The model was applied to several reactions induced by ^{6}He [17], showing in all cases a good agreement with the elastic data.

Recently, the CDCC method has been extended to four-body problems (i.e., three-body projectiles) by the groups at Kyushu [18,10] and Seville [19,11,12]. The method has been applied so far to ^{6}He scattering, showing in most cases a very good agreement with the existing data.

In Fig. 1 we illustrate some examples of the application of the CDCC method to ^{6}He elastic scattering. The data correspond to the reactions ^{6}He + ^{64}Zn at 10 and 13.6 MeV [2] and ^{6}He + ^{208}Pb at 22 MeV [6] and 27 MeV [4]. The solid lines correspond to the four-body CDCC (4b-CDCC) calculations, quoted from Refs. [12,**?**]. Except for the ^{6}He + ^{64}Zn reaction at $E = 10$ MeV, where the calculation underpredicts the data, the agreement is very good. We include also in this figure the three-body CDCC (3b-CDCC) calculations performed with the improved di-neutron model described above (dashed lines) as well as the 3b-CDCC calculation omitting the coupling to the breakup channels (dotted lines). The ingredients of these calculations (two-body potentials, continuum discretization, etc) are the same as in [17], with the exception of the $2n-$target interaction. In [17], this interaction was approximated by a deuteron optical potential, while in the calculations shown here, this is calculated from the neutron-target optical potential with the following single-folding formula:

$$U(\mathbf{R}) = \int \rho_{nn}(r_{nn}) \left[U_n\left(\mathbf{R} + \frac{\mathbf{r}_{nn}}{2}\right) + U_n\left(\mathbf{R} - \frac{\mathbf{r}_{nn}}{2}\right)\right] d\mathbf{r}_{nn} \quad (1)$$

where U_n is the neutron-target optical potential evaluated at the appropriate energy per nucleon and $\rho_{nn}(r)$ is the $n-n$ density in the ground state of ^{6}He, that is, the probability of finding the two halo neutrons separated by a distance r within the ^{6}He nucleus. This density was calculated from the three-body wave function of ^{6}He used in the four-body CDCC calculations. Although the approximation of the $2n-$target interaction by a deuteron optical potential gives results in good agreement with the data [17], the prescription given by Eq. (1) provides results in better agreement with the 4b-CDCC calculations.

Comparing the dotted line (no-continuum calculation) with the dashed line (full 3b-CDCC) in Fig. 1 we see that the inclusion of the breakup channels has a strong impact on the elastic cross section. The effect is more evident in the ^{208}Pb case, where the inclusion of these couplings produces the disappearance of the Fresnel peak. We see also that the agreement between the 3b- and 4b-CDCC calculations is remarkable, indicating that the former provides an useful and simple tool to describe the elastic scattering of Borromean nuclei.

Although the CDCC method has proven to be an accurate technique to study elastic scattering of weakly-bound few-body nuclei, it has been shown recently that similar results can be obtained using the Coupled-Reaction-Channels (CRC) formalism. We discuss this method in the next section, in the context of the breakup observables.

3 Breakup observables

Unlike the case of the elastic data, breakup data are much more scarce and, with a few exceptions (see eg. [20–22]), most of the available data correspond to inclusive reactions in which only the charged fragments (α-particles) are recorded. In principle, the CDCC method provides, in addition to the elastic cross section, the breakup ones. In the case of ^{6}He, 3b-CDCC calculations based on the di-neutron model described in the previous section, have been able to describe well the exclusive breakup data of Aumann *et al.* [20] for the ^{6}He + ^{208}Pb and ^{6}He + ^{12}C reactions [23].

However, comparison of available inclusive data with CDCC calculations [24–26] shows that, although these calculations reproduce very well the elastic data for these reactions, they tend to underestimate the α yield. A possible reason for this underestimation is the fact that the CDCC method provides only the so-called *elastic breakup* cross section, that is, the breakup in which the fragments resulting from the dissociation of the projectile are not absorbed by the target and the latter remains in its ground state. Since the neutrons are not detected in these experiments, these data may contain events in which the neutrons are transferred to the target or in which the target is excited.

In Ref. [25], we showed that a useful procedure to take into account, at least partially, these events is by means of the *transfer to the continuum* (TC) approach [27,28], in which the halo neutrons are assumed to be transferred to bound and unbound states states of the target nucleus. On the other hand, the CDCC method relies on a *direct breakup* (DBU) picture, in which the ^{6}He dissociation is treated as an inelastic excitation of the projectile to its continuum spectrum. If the states included in the TC calculations are limited excitation energies above the $2n$ breakup threshold, one would expect both methods to provide the same results for the breakup cross sections, provide that the

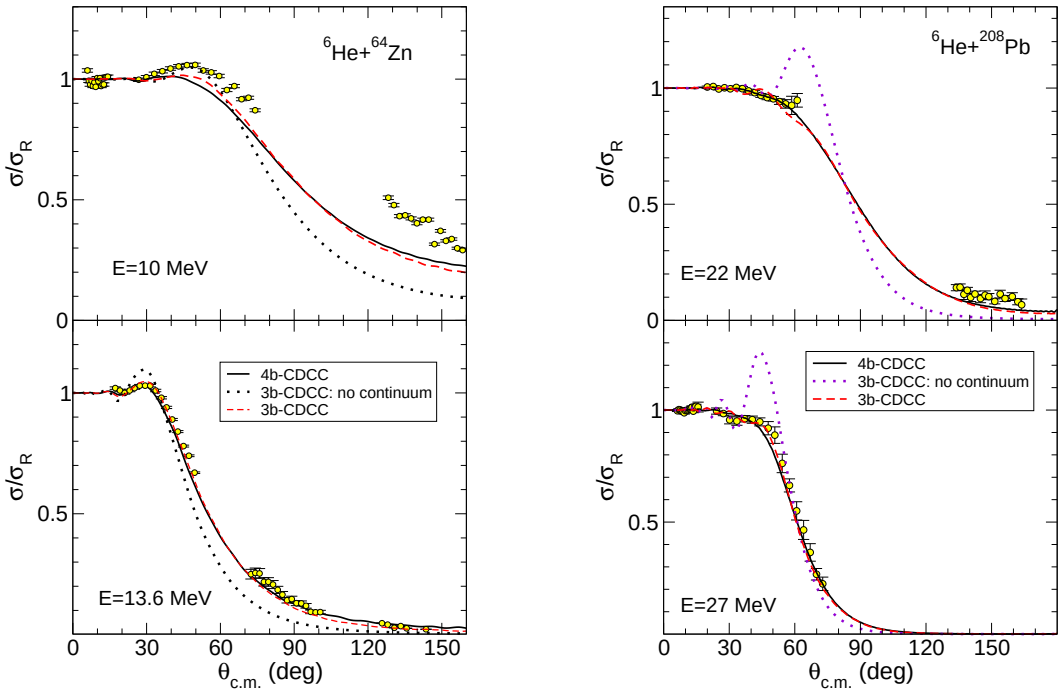

Fig. 1. Three- and four-body CDCC calculations for the elastic scattering for the reactions ^{6}He + ^{64}Zn (left) and ^{6}He + ^{208}Pb (right). The data are from Refs. [2] and [4,6], respectively.

underlying interactions are the same and the model space is sufficiently large to achieve convergence of the studied observables [28]. In this respect, the direct breakup and transfer to the continuum methods would be just alternative approaches to describe the projectile dissociation. However, in the TC scheme one can include also states below this threshold, which will be absent from the representation in terms of the states of the projectile.

In the TC calculations one should consider, in principle, both the 1n and 2n transfer channels. Since the f nal states populated by these two mechanisms are not mutually orthogonal, a simultaneous inclusion of both sets of f nal states has to be done with caution to avoid double-counting. Moreover, 2n transfer channels can proceed via a direct mechanism or a sequential mechanism. Therefore, the one-neutron transfer would also contribute as a f rst step to the 2n transfer. Since we are not interested here in the specif c states populated in this process, we believe that for the purposes of estimating the inclusive α yield it is sufficient to include a complete representation of the states that are accessible in the process. These states are not necessarily the physical states populated in the reaction. They should be rather considered as *doorway states* to which the halo neutrons are transferred. In the TC calculations presented in [25] for the ^{6}He + ^{208}Pb reaction, we considered separately the 1n and 2n mechanisms, and found that the latter provides a better description for the α-particles measured at large angles. For each value of the relative angular momentum between the tranferred pair and the ^{208}Pb core we consider a set of doorway states, distributed in a range of excitation energies of ^{210}Pb system. These representative states include both, bound and unbound states, with respect to the two-neutron breakup threshold. Above this threshold, the 2n-^{208}Pb continuum was discretized using energy bins, as done in the CDCC method.

As an example, we compare in Fig. 2 the measured energy distribution for α particles produced in the ^{6}He+^{208}Pb reaction at $E_{\rm lab}$ = 22 MeV between $\theta_{\rm lab}$ = 132° and 164°, with the TC calculations (dashed line). In these calculation, the transfer couplings were treated in DWBA. The calculation reproduces rather well the shape of the distribution. The absolute magnitude is somewhat underestimated, but this discrepancy might be well attributed to our approximate representation for the ^{210}Pb states. Also shown in this f gure is the 3b-CDCC calculation (dotted-dashed line), which largely underestimates the data.

In a recent work [26], we have also studied the effect of the transfer channels on the elastic cross section. This requires the inclusion of the transfer couplings beyond the Born approximation, thus performing a Coupled Reaction Channels (CRC) calculation. In the DWBA calculations of Ref. [25], the entrance channel was described by an optical potential f tted to the elastic data. This optical potential takes into account, in an effective way, the effects of channel couplings in the elastic cross section. In the CRC calculations, these couplings are taken into account explicitly and therefore the entrance channel is described by a *bare* interaction, that is, a potential that represents the interaction between the colliding nuclei in absence of couplings. For this bare interaction we took the São Paulo double-folding potential (SPP) [29,30]. We recall that some of these transfer channels correspond to unbound states of the f nal nucleus and, therefore, they can be identif ed with breakup.

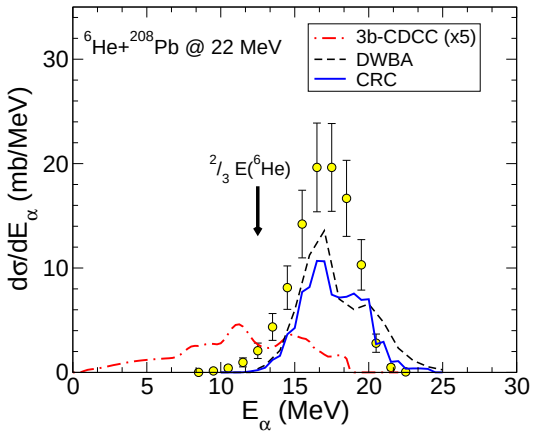

Fig. 2. Energy distribution of the α particles produced in the reaction ^{6}He+^{208}Pb at $E_{\rm lab}$ = 22 MeV, integrated in the angular interval $\theta_{\rm lab}$ = 132° − 164°. The dashed, dotted-dashed and solid lines are DWBA, CDCC and CRC calculations, respectively. The experimental data are from Ref. [25].

In Fig. 3 (right) we compare the elastic cross section, obtained from these CRC calculations, with the experimental data for the reaction ^{6}He + ^{208}Pb at 22 and 27 MeV. For comparison, the 3b-CDCC calculation, based on the same di-neutron model, is also shown. The agreement between both calculations is noticeable. A similar degree of agreement between both approaches was observed at the other energies of the experiment [26]. Therefore, the inclusion of the transfer channels produces essentially the same effect on the elastic cross section as the inclusion of the ^{6}He continuum states in the CDCC calculations. This result supports the idea that both methods populate to a large extent the same f nal states, although these states are expressed in different basis representations. We have included also the one-channel calculation performed with the bare interaction. The sizable difference between this calculation and the data ref ects once more the importance of the coupling to the transfer/breakup channels.

The α energy distribution predicted by the CRC calculation at $E_{\rm lab}$ = 22 MeV is shown in Fig. 2 (solid line). This calculation is similar to the DWBA result (dashed line); it describes well the shape of the data but underpredicts somewhat the absolute value. The similitude between the DWBA and CRC results indicate that multi-step processes, which are indeed very important, are well accounted for in the DWBA calculation by the phenomenological optical potential adjusted to the elastic scattering data. We emphasize that, unlike the DWBA calculations, the CRC calculations are able of reproducing simultaneously the elastic and α production channels without requiring any phenomenological f t of the elastic cross section.

In order to assess the validity of this approach in other situations, we have also performed a CRC analysis of the ^{6}He + ^{64}Zn reaction. As in the ^{6}He + ^{208}Pb case, the α events measured in this experiment are inclusive with respect to the f nal states of the removed neutrons. Therefore, transfer and breakup channels appear entangled in the data. Following the approach used in the ^{6}He + ^{208}Pb reaction, we consider the transfer of the halo neutrons to bound as well as unbound states of the target nucleus. In this case, we found that the 1n transfer mechanism provides a more suitable representation. We emphasize that, since the f nal states populated by 1n and 2n transfer are not orthogonal, our calculations may contain also contribution from 2n transfer. A possible representation for the ^{65}Zn f nal states would be the physical states populated, for example, in ^{64}Zn(d, p)^{65}Zn reactions. However, there are very few studies of this kind in the literature and the spectroscopic information provided by these studies is limited to a few low-lying states of the ^{65}Zn nucleus. For example, in the (d, p) measurements of Lin and Cohen [31], only ^{65}Zn states below ∼ 5 MeV where identif ed and analyzed. When summing the spectroscopic factors for these states, one f nds [31] that a signif cant part of the single-particle strength for the identif ed orbitals is missing from the data. Aside from the usual uncertainties inherent to the determination of absolute spectroscopic factors from transfer reactions, this result suggests that, if one restricts the basis representation to the states identif ed by Lin and Cohen, one may miss a signif cant fraction of the inclusive cross section. So, our set of f nal states includes the single-particle states reported in [31], plus some additional *doorway states* which are intended to account for the remaining single-particle strength. To estimate the position of these doorway states we have performed a mean-f eld calculation of the ^{65}Zn nucleus, using the Skyrme Sk20 interaction. Further details of these calculations will be provided in a forthcoming publication.

These CRC calculations are compared in Fig. 3 (left) with the elastic data of Di Pietro *et al.* [2] and with the 3b-CDCC results (dashed lines). The dotted line is the one-channel calculation obtained with the bare potential alone. It is seen that the inclusion of the transfer channels produces a sizable reduction of the elastic cross section at the rainbow region and, in the case of the 13.6 MeV data, a slight increase at backward angles. Although the CDCC and CRC calculations are in reasonable agreement, the CRC cross section is larger at the maximum, which might be a consequence of the lack of completeness of the basis representation for the f nal states of the residual nucleus.

4 Fusion cross section

The two methods used here, namely, the CDCC and the CRC, have been used by several authors to calculate the fusion cross section (see for instance [32–34]). In both approaches, the complete fusion cross section is evaluated as the absorption of a short-range imaginary potential added to the projectile-target interaction. The CDCC approach has the limitation of excluding the rearrangement channels and, therefore, the possible inf uence of these states on the fusion probability. In this respect, the CRC method seems to provide a more suitable approach to calculate fusion (see [33] for a recent review).

In this section, we discuss the fusion cross section provided by the CRC calculations described in the preceding section and compare them with available data. Fol-

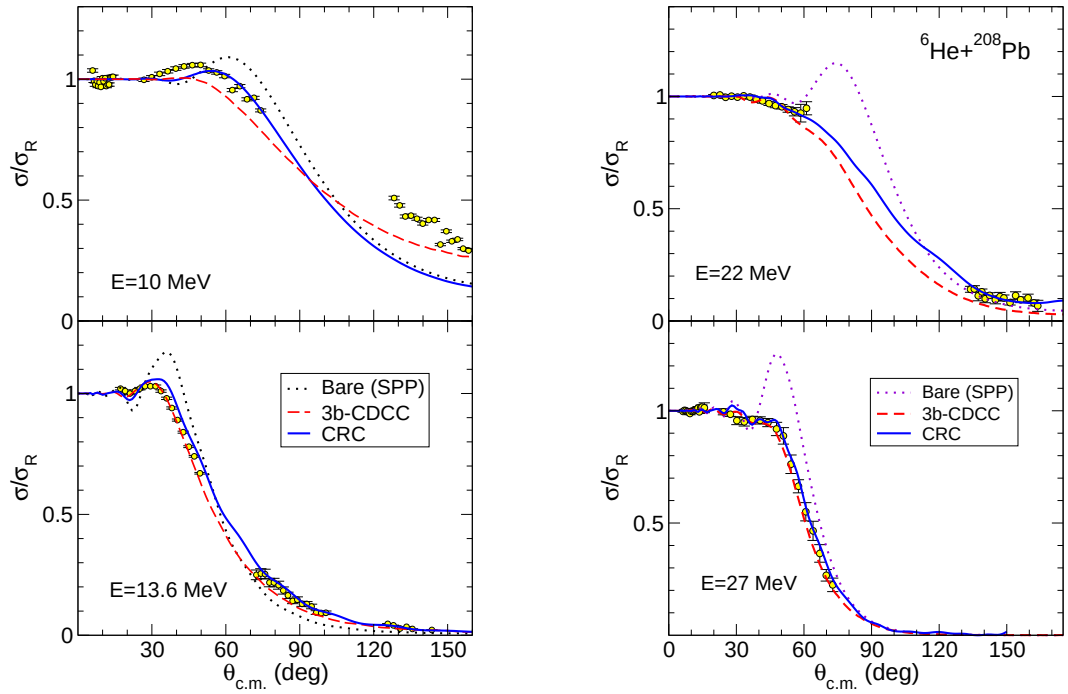

Fig. 3. CRC calculations for the ^{6}He + ^{64}Zn (left) and ^{6}He + ^{208}Pb (right) reactions. For each panel, the dotted line is the one-channel calculation performed with the bare interaction, the dashed line is the three-body CDCC calculation and the solid line is the CRC calculation.

lowing the standard procedure, we include a short-range imaginary potential of Woods-Saxon form with parameters $W = 50$ MeV, $R_0 = 1.0 \times (A_p^{1/3} + A_t^{1/3})$ fm and $a_0 = 0.1$ fm and identify the total fusion cross section with the absorption due to this potential.

In Fig. 4 we compare the calculated fusion excitation functions with the experimental data. Since the fusion for the ^{6}He + ^{208}Pb reaction has not been measured, we compare with the total fusion data for ^{6}He + ^{209}Bi measured by Kolata *et al.* [35]. The dashed line is the fusion calculated in absence of transfer/breakup couplings (i.e. with the bare interaction and the short-range imaginary potential) and the solid line is the CRC result.

Inclusion of the transfer channels, within the CRC formalism, produces a sizable hindrance of the fusion probability at energies above the Coulomb barrier, consistent with previous results [34]. In both cases, the CRC calculations are in reasonable agreement with the data. However, we found that the calculated fusion cross section is very sensitive to the assumed rms matter radius of the colliding nuclei. The densities used in these calculations use: 2.4 fm (^{6}He), 3.91 fm (^{64}Zn), and 5.67 fm (^{208}Pb). A more detailed study of this density dependence is left for a separate publication.

Notwithstanding these considerations, our calculations clearly indicate that the inclusion of transfer channels suppresses the fusion probability at energies above the Coulomb barrier. Below the barrier, the calculations do not show any clear evidence of suppression or enhancement.

5 Summary and conclusions

In this work we have discussed recent advances in the application of the CDCC and CRC methods to describe nuclear collisions involving loosely bound nuclei. The discussion and the applications have been focused on reactions induced by the ^{6}He nucleus at energies around the Coulomb barrier. We have studied the effect of the weak binding of this nucleus on elastic, transfer/breakup and fusion.

The elastic scattering is suitably studied with the CDCC approach, in which the coupling to the breakup channels is treated in terms of inelastic excitations to the ^{6}He continuum. We have compared three- and four-body CDCC calculations which make use, respectively, of a two-body ($\alpha + 2n$) or three-body ($\alpha + n + n$) model of ^{6}He. In the former case, the parameters of the model are chosen in order to mimic in the best possible way the $\alpha - 2n$ density, according to a three-body calculation of ^{6}He. Both types of CDCC calculations describe pretty well the data for the reactions considered.

Despite their success to describe the elastic data, the CDCC calculations fail to describe the inclusive α cross sections. For these observables, we have shown that the CRC method provides a more suitable approach. In this method, the ^{6}He dissociation is treated within a transfer to the continuum picture, assuming a $1n$ or $2n$ transfer mechanism. Unlike the CDCC method, the CRC method permits the inclusion of transfer to bound states of the target nucleus.

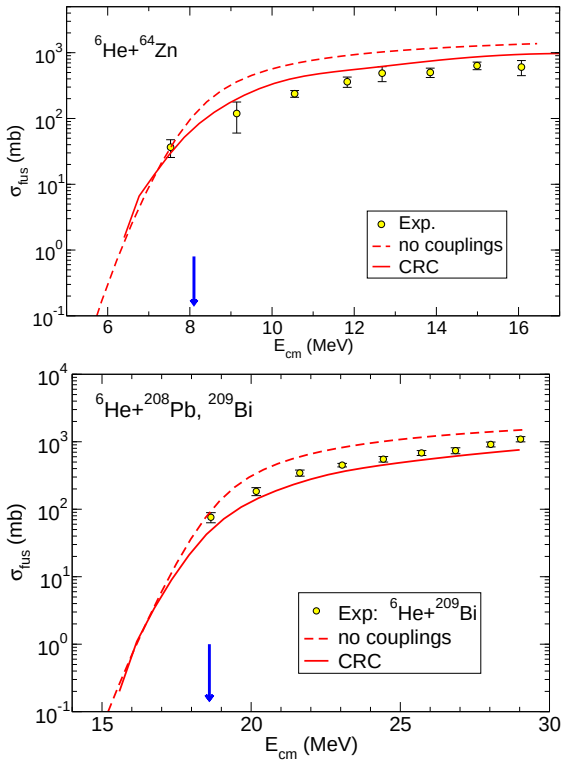

Fig. 4. Fusion excitation function for the reactions ^{6}He + ^{64}Zn (top) and ^{6}He + ^{208}Pb (bottom) obtained with the CRC method. The ^{64}Zn data are from Ref. [2]. The data in the bottom panel, correspond to the fusion for ^{6}He + ^{209}Bi [35]. The vertical arrows indicate the position of the nominal Coulomb barrier.

We have also explored the possibility of calculating fusion cross sections within the CRC method. As in other works, the complete fusion cross section is estimated as the absorption of a short-range imaginary potential added to the bare interaction. We have applied this method to the ^{6}He+^{208}Pb and ^{6}He+^{64}Zn reactions. In both cases, the calculation indicates that the inclusion of the transfer/breakup channels produces a signif cant suppression of the fusion probability at energies above the Coulomb barrier, improving the agreement with the data.

We are grateful to A. Di Pietro and V. Scuderi for providing us the ^{6}He + ^{64}Zn data and to E.F. Aguilera and J. Kolata for the ^{6}He+^{209}Bi data, and for useful discussions concerning their interpretation. This project has been partially supported by the Spanish Ministerio de Ciencia e Innovación under project FPA2009-07653 and by the Spanish Consolider-Ingenio 2010 Programme CPAN (CSD2007-00042).

References

1. E.A. Benjamim et al., Phys. Lett. B **647**, 30 (2007)
2. A. Di Pietro et al., Phys. Rev. C **69**, 044613 (2004)
3. P.N. de Faria et al., Phys. Rev. C **81**, 044605 (2010)
4. O.R. Kakuee et al., Nucl. Phys. **A728**, 339 (2003)
5. O.R. Kakuee et al., Nucl. Phys. **A765**, 294 (2006)
6. A.M. Sánchez-Benítez et al., Nucl. Phys. **A803**, 30 (2008)
7. E.F. Aguilera et al., Phys. Rev. Lett. **84**, 5058 (2000)
8. E.F. Aguilera et al., Phys. Rev. C **63**, 061603 (2001)
9. N. Austern, Y. Iseri, M. Kamimura, M. Kawai, G. Rawitscher, M. Yahiro, Phys. Rep. **154**, 125 (1987)
10. T. Matsumoto, T. Egami, K. Ogata, Y. Iseri, M. Kamimura, M. Yahiro, Phys. Rev. C **73**, 051602(R) (2006)
11. M. Rodríguez-Gallardo, J.M. Arias, J. Gómez-Camacho, R.C. Johnson, A.M. Moro, I.J. Thompson, J.A. Tostevin, Phys. Rev. C **77**, 064609 (2008)
12. M. Rodríguez-Gallardo, J.M. Arias, J. Gómez-Camacho, A.M. Moro, I.J. Thompson, J.A. Tostevin, Phys. Rev. C **80**, 051601(R) (2009)
13. K. Rusek, K.W. Kemper, R. Wolski, Phys. Rev. C **64**, 044602 (2001)
14. R.S. Mackintosh, K. Rusek, Phys. Rev. C **67**(3), 034607 (2003)
15. K. Rusek, N. Alamanos, N. Keeley, V. Lapoux, A. Pakou, Phys. Rev. C **70**(1), 014603 (2004)
16. K. Rusek, I. Martel, J. Gómez-Camacho, A.M. Moro, R. Raabe, Phys. Rev. C **72**, 037603 (2005)
17. A.M. Moro, K. Rusek, J.M. Arias, J. Gómez-Camacho, M. Rodríguez-Gallardo, Phys. Rev. C **75**, 064607 (2007)
18. T. Matsumoto, E. Hiyama, K. Ogata, Y. Iseri, M. Kamimura, S. Chiba, M. Yahiro, Phys. Rev. C **70**, 061601(R) (2004)
19. M. Rodríguez-Gallardo, J.M. Arias, J. Gómez-Camacho, R.C. Johnson, A.M. Moro, I.J. Thompson, J.A. Tostevin, Eur. Phys. J. S.T. **150**, 51 (2007)
20. T. Aumann et al., Phys. Rev. C **59**, 1252 (1999)
21. P.A. DeYoung et al., Phys. Rev. C **71**, 051601(R) (2005)
22. A. Chatterjee et al., Phys. Rev. Lett. **101**(3), 032701 (2008)
23. J.A. Lay, A.M. Moro, J.M. Arias, J. Gómez-Camacho, Phys. Rev. C **82**, 024605 (2010)
24. P.N. de Faria et al., Phys. Rev. C **82**, 034602 (2010)
25. D. Escrig et al., Nucl. Phys. **A792**, 2 (2007)
26. J.P. Fernández-García, M.A.G. Alvarez, A.M. Moro, M. Rodríguez-Gallardo, Phys. Lett. B **693**, 310 (2010)
27. A.M. Moro, R. Crespo, H. García-Martínez, E.F. Aguilera, E. Martínez-Quiroz, J. Gómez-Camacho, F.M. Nunes, Phys. Rev. C **68**, 034614 (2003)
28. A.M. Moro, F.M. Nunes, Nucl. Phys. **A767**, 138 (2006)
29. L.C. Chamon et al., Phys. Rev. C **66**, 014610 (2002)
30. L.C. Chamon, D. Pereira, M.S. Hussein, M. Cândido-Ribeiro, D. Galetti, Phys. Rev. Lett. **79**, 5218 (1997)
31. E.K. Lin, B.L. Cohen, Phys. Rev. **132**, 2632 (1963)
32. A. Diaz-Torres, I.J. Thompson, Phys. Rev. **C65**, 024606 (2002)
33. N. Keeley, R. Raabe, N. Alamanos, J.L. Sida, Prog. Part. Nucl. Phys. **59**, 579 (2007)
34. N. Keeley, N. Alamanos, Phys. Rev. C **77**, 054602 (2008)
35. J.J. Kolata et al., Phys. Rev. Lett. **81**, 4580 (1998)